UDC 544.653.2/3

COMPARATIVE ELECTROCHEMICAL CHARACTERISTICS OF PURE AND ALUMINUM-DOPED LiMn$_2$O$_4$ CATHODE MATERIALS FOR LITHIUM-ION BATTERIES

V. KOSILOV, Y. KRAVETS
Joint Department of Electrochemical Energy Systems
3s23p2@bigmir.net

In this paper, regularities of overstoichiometric lithiation of LiMn$_2$O$_4$ spinel samples of different origin have been established using the methods of galvanostatic (CCCV) and voltammetric cycling. Unlike individual LiMn$_2$O$_4$, the aluminum doped spinel reveals high stability after repeated overdischarge. In particular, individual LiMn$_2$O$_4$ does not tolerate even a few individual overdischarge cycles of the cathode below 3.0 V, whereas several overdischarge cycles are not critical for the aluminum doped spinel.

The lithium manganese spinel LiMn$_2$O$_4$ has been known since 1983 as a cathode material for lithium-ion batteries [1] and is the subject of numerous researches to this day [2,3]. The electrochemical intercalation/ deintercalation of lithium ions into/from the lattice of LiMn$_2$O$_4$ occurs at about 4 V according to eq. (1),

$$\text{LiMn}_2\text{O}_4 \leftrightarrow \text{Li}_{1-x}\text{Mn}_2\text{O}_4 + x\text{Li}^+ + x\text{e}^-. \tag{1}$$

The theoretical capacity of the spinel is 148 mAh·g^{-1}. In the composition ranges of $0 \leq x \leq 0.5$ and $0.5 \leq x \leq 1.0$, the reaction takes place in two stages, but the spinel keeps its cubic structure with the lattice parameter a=8.248 Å. These stages can be well observed on galvanostatic curves, which consist of two separated flat regions, and on cyclic voltammetry curves having two typical peaks corresponding with the intercalation/ deintercalation of lithium ions. At the same time, when lithium ions are in excess, x>1 (overlithiation), the intercalation potential of lithium ions becomes ~2.9 V to Li/Li$^+$, and the spinel structure experiences a tetragonal disorder with a small increase in the unit cell volume (a=8.007 Å, c=9.274 Å) according to reaction (2):

$$\text{Li} + \text{LiMn}_2\text{O}_4 \leftrightarrow 2\text{LiMnO}_2 \tag{2}$$

Furthermore, the Jahn-Teller effect contributes to this distortion. It can be observed during the accumulation of more than 50% of Mn^{3+} ions according to reaction (2) and results in the symmetry lowering of the structure [4]. Low cycling ability of lithium-ion batteries with LiMn$_2$O$_4$ cathodes, typical for reaction (2), is mainly due to the destruction of the cathode material because of its asymmetrical expansion/contraction

upon charging/discharging [5]. One of the ways to improve electrochemical characteristics of the lithium-manganese spinel is the substitution of manganese ions and obtaining compounds of a $LiMe_{1-x}Me_xO_4$ formula [6].

Reaction (2) can partly occur upon malfunctions in a battery operation, first of all, upon overdischarge. The effect of overdischarge (overlithiation) on the stoichiometric spinel $LiMn_2O_4$ prepared by different methods is well described [5]. In order to avoid overdischarge and the occurrence of reaction (2), charge-discharge cycling of doped spinels is conducted at discharge potentials above 3.0 V [7]. As lowering the charge/discharge voltage inevitably leads to overdischarge and overlithiation effects, the determination of the overlithiation mechanism and its role in various modifications of the lithium-manganese spinel is an important issue. Therefore the objectives of this research have been to establish the general pattern of overstoichiometric lithiation of $LiMn_2O_4$ and to study the effect of excess lithium intercalation on the following electrochemical behavior of manganese spinel in high voltage regions. From a practical point of view a long-term cycling of cathodes based on spinel materials in different potential ranges will allow to draw a conclusion about their stability to the overdischarge phenomena during exploitation of lithium-ion batteries.

Materials and methods

In this study, commercial samples of lithium-manganese spinel, viz., stoichiometric $LiMn_2O_4$ EQ-Lib-LMO by MTI (USA) and modified $LiMn_2O_4$ HPM-9051C by Toda Kogyo Corp. (Japan), containing 1.52% aluminum were used (Table 1).

Electrochemical studies were performed in sample button-type 2016 cells with lithium metal as a counter and reference electrode. A slurry was prepared by mixing the active material, Super P and SFG6 (Timcal) conductive additives, and a PVdF binder (Kureha #1100) in N-methylpyrrolidone (Sigma-Aldrich) with the "dry" component ratio of 80:7:5:8 in a high-speed mixer (IKA RW 20). The working electrode was made by coating the aluminum current collector with the slurry. The mass loading of the electrode was 4-5 mg/cm^2; it was pressed to the thickness of 17-20 μm. A 1M solution of $LiPF_6$ in a mixture of EC and DMC (1:1 by weight) was used as an electrolyte. The cells for cycling were assembled in an argon-filled glove box. Electrochemical experiments were conducted on a home-made automated electrochemical workstation using cycling voltammetry (CV) at the scan rate of 0.1 mV/s and galvanostatic cycling in CC and CCCV modes. The 146.7 mA/g current numerically equal to the theoretical discharge capacity of the stoichiometric $LiMn_2O_4$ was taken as 1.0C.

Table 1. Physical and chemical characteristic of LiMn$_2$O$_4$

	LiMn$_2$O$_4$ MTI EQ-Lib-LMO (USA)	LiMn$_2$O$_4$ Toda HPM-9051C(Japan)
Working range	3,4 – 4,5 V	3,4 – 4,3 V
Nominal capacity	115 mA·h/g	96 mA·h/g
Particle size	12 mkm	10 mkm
Specific surface	0,4~1,0 m^2/g	0,51 m^2/g

Before the main experiment, all samples underwent four formation cycles of galvanostatic charge/discharge cycling with a 0.1C current and three testing CV cycles with the scan rate of 0.1 mV/s. Testing CV cycles in the typical range of potentials were conducted between series with different final discharge potentials.

Results and Discussion

In preliminary CV tests (Fig. 1 A, B), characteristics of both electrode materials with the final intercalation potential of 1.5 V were obtained. First, electrode cycling in the standard range of potentials was conducted and typical CV characteristics (cycle 6) extensively described in literature [1-8] were acquired. The specific capacities of the stoichiometric spinel (MTI) and the aluminum-modified sample (Toda) are 115 mA·h/g and 91 mA·h/g, respectively.

Then cycling in the lower potential range (2.4-3.5 V) was performed. There were obtained a peak in the cathode region and a reverse peak in the anode region at around 2.9 V (cycle 9), corresponding to the Mn^{4+}↔Mn^{3+} red-ox reaction and to the transformation of the cubic phase to the tetragonal one [9]. Cycling in the 2.4-3.5 V range showed reverse capacity of about 80 and 46 mA·h/g for the MTI and Toda samples, respectively. After this, the electrodes were cycled in the typical potential range (cycle 12). A small decrease in peak current (and, respectively, capacity) in the regular spinel and a nearly complete reproducing of the curve in the modified LiMn$_2$O$_4$, compared to cycle 3, were observed.
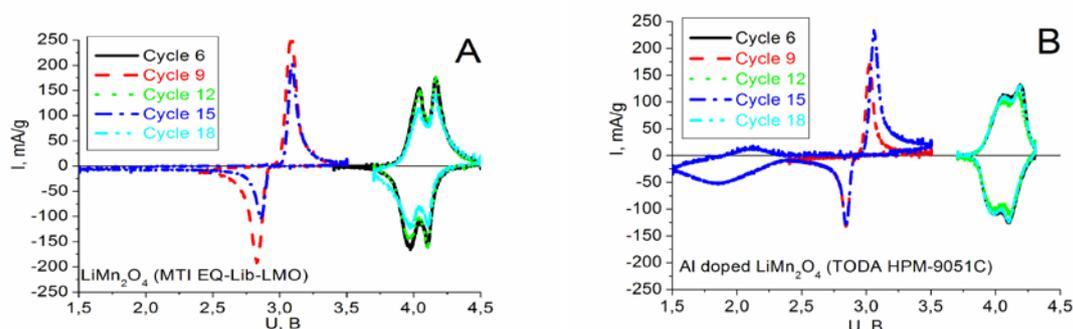
Figure 1. *CV curves of LiMn$_2$O$_4$ by MTI (A) and Toda (B) upon cycling to 2.4 and 1.5 V*

Further, electrodes were cycled in the potential range of 1.5 – 3.5 V imitating a deep overdischarge. The treatment of the MTI material to 1.5 V (Fig. 1A, cycle 15) showed a practically full absence of processes in the 1.5 – 2.4 V potential range. At the same time, CV characteristics in the standard potential range demonstrated a considerable decrease in peak current values (cycle 18) with a decrease in specific capacity to 94 mA·h/g.

A deeper intercalation to 1.5 V (Fig.1 B, cycle 13) showed a capacity up to 110-115 mA·h/g, with a wave at about 2.0 V, which disappears on the following cycles (curve 15). Interestingly, returning to the cycling potential range of 2.4 V – 3.5 V gave a twofold increase in capacity, from 46 to 94 mA·h/g. Test CV curves obtained in the higher-voltage region before and after the low-voltage treatment (curves 12 and 18), showed a minor decrease in specific capacity without the change of the curve shapes. This capacity drop can be explained, most likely, by the increase in the electrode resistance because of the growth of passive films during multiple cycles in the low-voltage range. The effect of increasing peak currents and specific capacity in the intercalation/deintercalation process in the potential region around 3.0 V after treatment until 1.5 V is presumably related to the structure features of the lithium-manganese spinel doped with aluminum, and requires additional physical, chemical and electrochemical investigations.
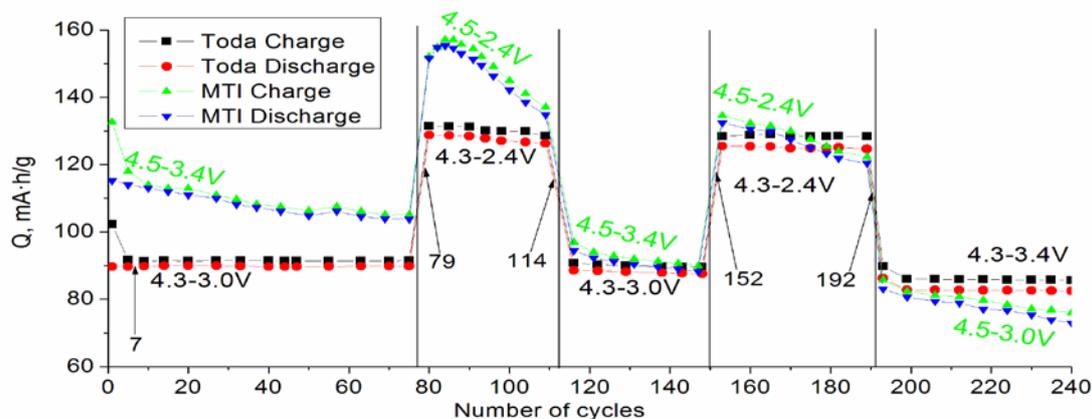
Figure 2. *Dependence of specific capacity in the lithium intercalation-deintercalation processes in LiMn$_2$O$_4$ by MTI (A) and Toda (B) during long-term cycling in different ranges of potentials. Numbered arrows refer to the number of the cycle in test CV measurements*

As a next step, a long-term resource cycling of MTI and Toda samples at standard working ranges (see Table 1) and with overdischarge to 2.4 V (Fig.2) was made. Cycling was held in the CCCV regime: charging with a 1.0C current, surcharging to 0.1C, and discharging at 1.0C. Between these regimes, CV measurements were carried out at a scan rate of 0.1 mV/s (Fig. 3 A, B).

40

As can be observed from Fig. 2, cycling of $LiMn_2O_4$ (MTI) to 3.4 V exhibits a decrease in specific capacity values, which equal to 105 mA·h/g after 75 cycles, whereas $LiMn_2O_4$ (Toda) holds a higher stability of electrochemical characteristics. The value of specific capacity while cycling in the standard range of potentials (4.3-3.0 V) during 75 cycles remains constant and is of about 90 mA·h/g.

As shown in Fig.2, decreasing the cycling voltage to 2.4 V (cycles 80-109) shows an increase in the specific capacity of $LiMn_2O_4$ (MTI) to 155 mA·h/g with the following rapid decline to 135 mA·h/g. For $LiMn_2O_4$ (Toda), widening the working potential range leads to smaller changes in specific capacity.

Returning to the 4.5-3.4 V cycling window (cycles 115-147) for $LiMn_2O_4$ (MTI) reveals a decrease in capacity compared to the starting cycling from 105 to 95 mA·h/g and to a further capacity decline with the speed of 0.17 mA·h/g per cycle. On the contrary, $LiMn_2O_4$ (Toda) in the standard cycling window restores its initial characteristics. Further cycling to lowest possible potentials (cycles 153-189) and within recommended potentials (cycles 193-240) supports the trend obtained.

CV measurements in the standard potential range conducted after each series of the resource cycling are shown in Fig. 3 A, B. It is evident that after cycling $LiMn_2O_4$ (MTI) to the final potential of 2.4 V a fast decrease in the peak current and current slope is observed. Fig. 4 reveals that the specific capacity values and the Coulomb efficiency of lithium intercalation/deintercalation are also decreasing.
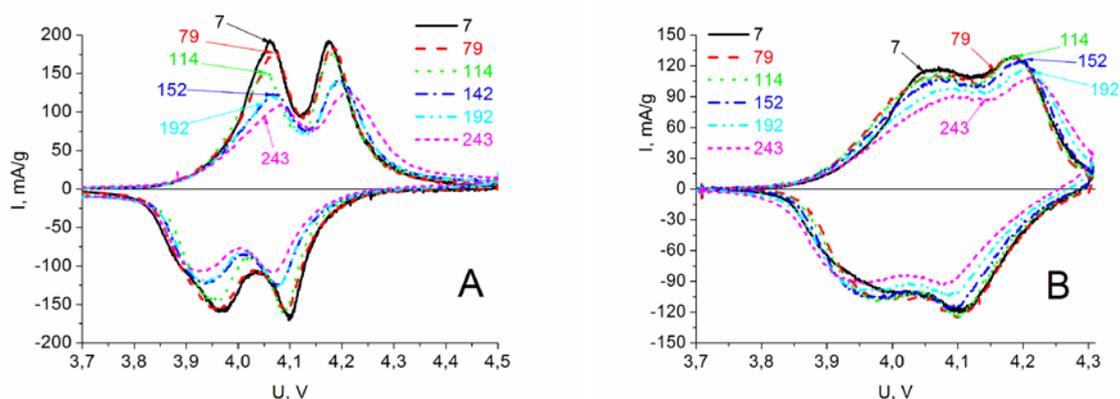
Figure 3. *CVs of $LiMn_2O_4$ by MTI (A) and Toda (B) on long-term cycling to different potentials according to conditions denoted in Fig.2.*

CV characteristics of $LiMn_2O_4$ (Toda) (Fig. 3 B) confirm conclusions regarding the dependence of capacity on cycle number. During more than 240 cycles, the shape of the CV curves remains constant. A decrease in the peak current and the current slope are observed since 190 cycles. At the same time, a decrease in the specific capacity and Coulomb efficiency is noticed.

Conclusions

Simulation of deep overdischarge during 240 cycles shows a high stability of the aluminum doped lithium-manganese spinel compared with the stoichiometric sample. From a practical point of view it can be stated that commercial $LiMn_2O_4$ (MTI) as a cathode material in lithium-ion batteries does not tolerate even a few overdischarge cycles at 3.0 V. On the contrary, the application of lowered discharge potentials to the aluminum doped $LiMn_2O_4$ (Toda) is not critical for its successful operation.

Acknowledgments

The authors are grateful to Mr S.I. Chernukhin for assistance and to Dr. S.A. Kirillov for discussions and comments.

References

[1]   Thackeray M.M., David W.I.F., Bruce P.G., Goodenough J.B., Lithium insertion into manganese spinels, Mater. Res. Bull., 18, 461-472 (1983).

[2]   Whittingham M.S., Lithium batteries and cathode materials, Chem. Rev., 104, 4271-4301 (2004).

[3]   Park O.K., Cho Y., Lee S., Yoo H-C., Song H-K., Cho J. Who will drive electric vehicles, olivine or spinel?, Energy Environ. Sci., 4, 1621-1633, (2011).

[4]   Yamada A., Lattice instability in $Li(Li_xMn_{2-x})O_4$, J. Solid State Chem., 122, 160–165 (1996).

[5]   Winter M., Besenhard J.O., Spahr M.E., Novak P., Insertion electrode materials for rechargeable lithium batteries, Adv. Mater. 10, 725-763 (1998).

[6]   Ohzuku T., Takeda S., Iwanaga M., Solid-state redox potentials for $Li[Me_{1/2}Mn_{3/2}]O_4$ (Me: 3d-transition metal) having spinel-framework structures: a series of 5 volt materials for advanced lithium-ion batteries, J. Power Sources, 81, 90-94 (1999).

[7]   Strobel P., Ibarra Palos A., Anne M. Structural, magnetic and lithium insertion properties of spinel-tipe $Li_2Mn_3MO_8$ oxides (M = Mg, Co, Ni, Cu), J. Materials Chem., 10, 429-436 (2000).

[8]   Xu H., Cheng B., Xu E., Xu L., Yang J., Qian Y., Investigations of high rate capability and high temperature performance for nano-sized porous $LiAl_xMn_{2-x}O_4$ (x=0, 0.05, 0.1, 0.15) cathode material, Int. J. Electrochem. Sci., 7, 11917 – 11929 (2012).

[9]   Potapenko A.V., Kirillov S.A., Lithium manganese spinel materials for high-rate electrochemical applications, J. Energy Chem., 23, 543–558 (2014).